R. Casasola, J. M. Pérez, M. Romero, Crystal growth of F-phlogopite from glasses of the SiO_2-Al_2O_3-MgO-K_2O-F system. *Journal of the American Ceramic Society, 99 (2016) 484-491*; doi:10.1111/jace.13995

Crystal growth of F-phlogopite from glasses of the SiO_2-Al_2O_3-MgO-K_2O-F system

Raquel Casasola, Juan M. Pérez, Maximina Romero*

Group of Glass and Ceramic Materials,
Eduardo Torroja Institute for Construction Sciences, IETcc-CSIC
C/ Serrano Galvache 4. 28033 Madrid. Spain.

* Corresponding author, Tel.: +34 91 302 04 40; Fax: + 34 91 302 07 00.
e-mail address: mromero@ietcc.csic.es

iAbstract

A study on the devitrification of fluorophyllosilicate glass precursors is presented. The research has been focused on the early stages of the crystallization process and shows the variation in the crystallization mechanism with increasing the fluorine content. The devitrification process has been studied by means of differential scanning calorimetry (DSC) and field emission scanning electron microscopy (FESEM). These complementary techniques established that both surface (heterogeneous nucleation) and volume (internal homogeneous nucleation) mechanisms are present in the crystallization process of fluorophlogopite-based glasses, the latter being predominant. By increasing the percentage of fluorine in the parent glass, a variation in the location of the first crystals developed from the internal volume of the glass towards the external surface was observed. Such an alteration in the crystallization mechanism was also checked by examining the microstructure of crystallized samples prepared under short time treatments.

Keywords: F-phlogopite; DSC; FESEM; crystallization mechanism; surface crystallization; bulk crystallization; microstructure.

1. Introduction

Glass-ceramics are ceramic materials consisting of at least one glass phase and one crystalline phase. Glass-ceramics are processed using controlled crystallization (nucleation and crystal growth) of a base glass. The great variety of compositions and the possibility of developing special microstructures with specific technological properties have allowed glass-ceramic

materials to be used in a wide range of applications[1-6]. By precipitating crystalline phases in the base glass, exceptional features can be achieved; e.g., mica glass-ceramics show unique machinable properties related to the cleavage of plate-like mica crystals.

Fluorphlogopite (henceforth, F-phlogopite) is a phyllosilicate with the empirical formula $KMg_3(Si_3Al)O_{10}F_2$, which shows a lamellar structure of trioctahedral mica[7]. Glass-ceramics containing F-phlogopite have been developed for multiple applications, such as machinable materials[8-10], biomaterials[11,12], Nicalon™ fiber reinforcement[13] and ceramic tile glazes[14].

The microstructure of F-phlogopite based glass-ceramics is characterized by cross-linked mica flakes that are immersed in a residual glass matrix[15-18]. The microstructure is an important factor to control in the design of glass-ceramics materials because most mechanical and optical properties are related to this feature, and it can promote or diminish the characteristics of glass-ceramics[3,19-24].

It is well known that fluorine plays a major role on the nucleation of F-phlogopite glasses[25-27]. However, to our knowledge, there has been no attempt to address the effect of fluorine on the progress of crystals at the first steps of devitrification of F-phlogopite glasses.

In a recent paper, the authors showed that the volume crystallization mechanism is prevalent in the devitrification process of F-phlogopite-based glasses[28]. Nevertheless, the increase of fluorine content in the glass composition changes the location of the first developed crystals from the internal volume of the glass particle to the surface sites. The present paper aims to study the crystal growth of glasses in the SiO_2-Al_2O_3-MgO-K_2O-F system with variable fluorine content.

2. Experimental

A glass in the SiO_2-Al_2O_3-MgO-K_2O-F system with the stoichiometric composition of F-phlogopite ($KMg_3(Si_3AlO_{10})F_2$), which is hereafter designated as FE glass, was formulated based on reagent-grade Al_2O_3, $(MgCO_3)_4Mg(OH)_2{\cdot}5H_2O$, K_2CO_3, MgF_2 and silica sand with low iron oxide contents. Based on the composition of FE glass two additional glass compositions were formulated, which contained 10 and 12 wt. % of fluorine in the starting batch, and were designated as F10 and F12, respectively.

The mixtures of raw materials were homogenized in a planetary ball mill (TURBULA) for 15 min. The batches were placed in alumina-silica crucibles and subsequently melted at 1450ºC for 2 h in an electric furnace. Frit glasses were obtained by pouring the melts into cool water. The

chemical analysis of the resulting glasses was determined with X-ray fluorescence (XRF) using a BRUCKER S8 Tiger spectrometer. The analysis was performed on pressed pellets of powder glass samples (<63 μm).

The crystallization mechanism was studied using both differential scanning calorimetry (DSC) and scanning electron microscopy with field emission cathode (FESEM). DSC runs were performed in a SETARAM Labsys Thermal Analyzer. The samples were heated from room temperature to 1400ºC at a heating rate of $50K \cdot min^{-1}$ under flowing air. Samples of ~40 mg were placed in platinum crucibles, and calcined Al_2O_3 was used as the reference material. All DSC curves were normalized with respect to the sample weight.

FESEM observations on cross sections of thermally treated frit glass samples were achieved with a HITACHI S-4800P microscope using an acceleration voltage of 20 kV. Glass-ceramic samples were polished to a 1 μm finish using diamond pastes after initially grinding with SiC powder. The samples were subsequently etched for 10 s in a solution of 5% HF, ultrasonically washed with distilled water and ethylic alcohol, dried and coated with Au-Pd in a Balzers SCD 050 sputter coater. A semi-quantitative analysis of different phases was performed using energy dispersive X-ray spectroscopy (EDS) with a Link eXL detector, which was provided by a beryllium (Be) window. The distribution of F, Mg, K, Si and Al among different crystalline phases was determined using digital X-ray mapping; this imaging technique is used to examine the two-dimensional distribution of elements in a specimen. Each two-dimensional map represents a single element, and the color variations on the map represent differences in weight percent of the elements from point to point.

3. Results and Discussion

The melts cooled in water led to homogeneous, transparent and free of defect frits. Table 1 shows the chemical composition that was determined by X-ray fluorescence of the investigated glasses.

During the melting process, the molten glass turned to be enriched in silica and alumina because the melt corroded the refractory crucibles (silico-alumina), which were used in melting the raw-material mixtures[29]. Simultaneously, the fluorine percentage is significantly reduced. Previous studies have shown that the loss of fluorine from alkali silicate melts containing fluorine additives is likely to occur simultaneously in the form of both alkalimetal fluoride (KF) and

silicon tetrafluoride (SiF_4)[30-34]. A detailed explanation of the change in chemical composition during melting of these glasses can be found in a previous work[28].

Table 1. Chemical composition (wt. %) of the investigated glasses determined by XRF (the errors are approximately ± 0.2 wt. %).

	FE	F-10	F-12
SiO_2	44.09	44.05	44.28
Al_2O_3	16.85	17.04	17.47
MgO	24.85	24.32	24.47
K_2O	9.72	9.68	8.09
F_2	4.49	4.91	5.69

The thermal behavior of FE, F10 and F12 glasses was evaluated with DSC in samples with two different particle sizes, i.e., fine (<63 μm powder) and coarse (~3x3x4 mm bulk). All of the thermograms show two exothermic peaks, which indicates that subsequent heat treatments can devtrify these glasses. For example, Figure 1 shows the recorded DSC curves of the FE glass.

The crystallization of a glass to develop a glass-ceramic material consists of a nucleation stage, in which small seeds or nuclei develop within the glass, followed by crystal growth step at higher temperature, which facilitates the enlargement of crystals. The development of crystalline phases can take place through two different mechanisms, i.e., volume and surface. In volume crystallization, the nuclei developed in the nucleation stage are homogeneously and randomly distributed throughout the whole volume of the glass. In surface mechanism, the crystallization starts from low energy surface sites (e.g., cracks, scratches, defects, foreign particles, etc.) and subsequently the crystals grow into the glass volume.

The nucleation of crystalline phases can occur through homogeneous nucleation, when the nuclei arise from their own melt composition in the absence of foreign boundaries, or heterogeneous nucleation, when crystalline phases develop from foreign boundaries, such as grain borders or interfaces

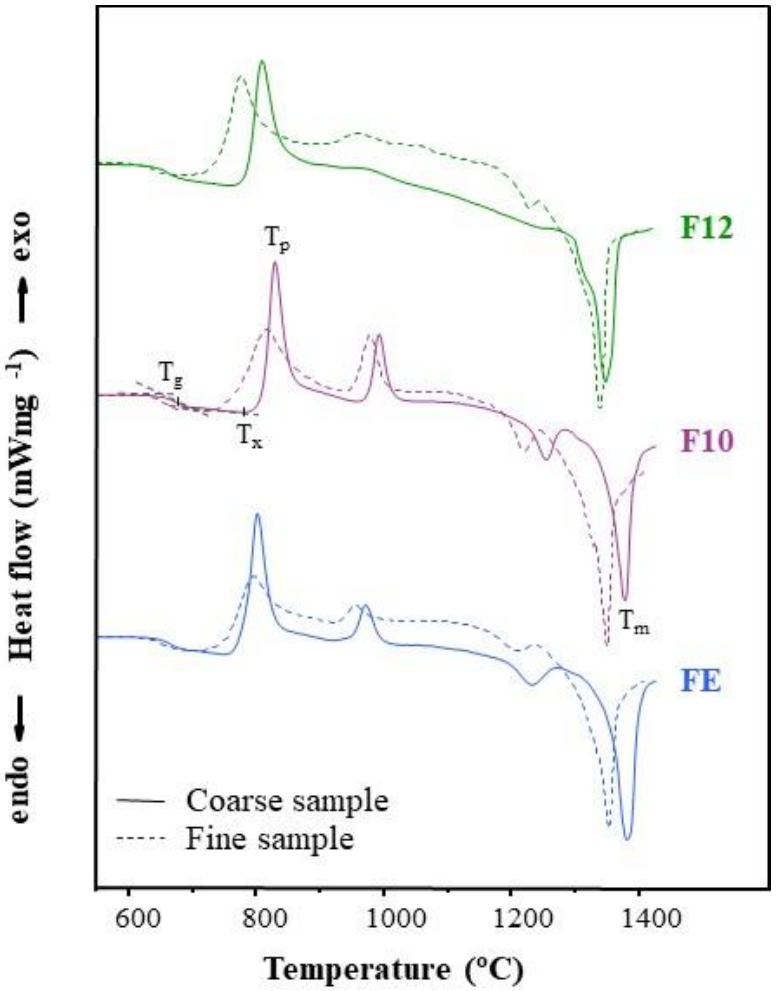

Figure 1. DSC curves from fine (<63 μm) and coarse samples for FE, F10 and F12 glasses.

The preferred crystallization mechanism (surface or volume) by which these F-phlogopite-based glasses devitrify was evaluated from the relative positions of the characteristic temperatures, which were obtained from DSC curves: glass transition temperature (T_g), onset and peak crystallization temperatures (T_x and T_p, respectively), and melting temperature (T_m), which is the temperature at the minimum of the endothermic peak.

The spatial position where the crystal nuclei are developed in the early stages of the crystallization process can be evaluated based on the values of ΔT_p, which indicate the crystallization temperature difference between fine and coarse glass samples ($\Delta T_p = T_{p(fine)} - T_{p(coarse)}$)[35]. Thus, the devitrification of glasses with $\Delta T_p > 0$ begins with the growth of crystals in the bulk of the glass particles, whereas $\Delta T_p < 0$ indicates that the first crystal nuclei will develop on the surface of the glass grains. Figure 2 shows the evolution of ΔT_p with the fluorine content.

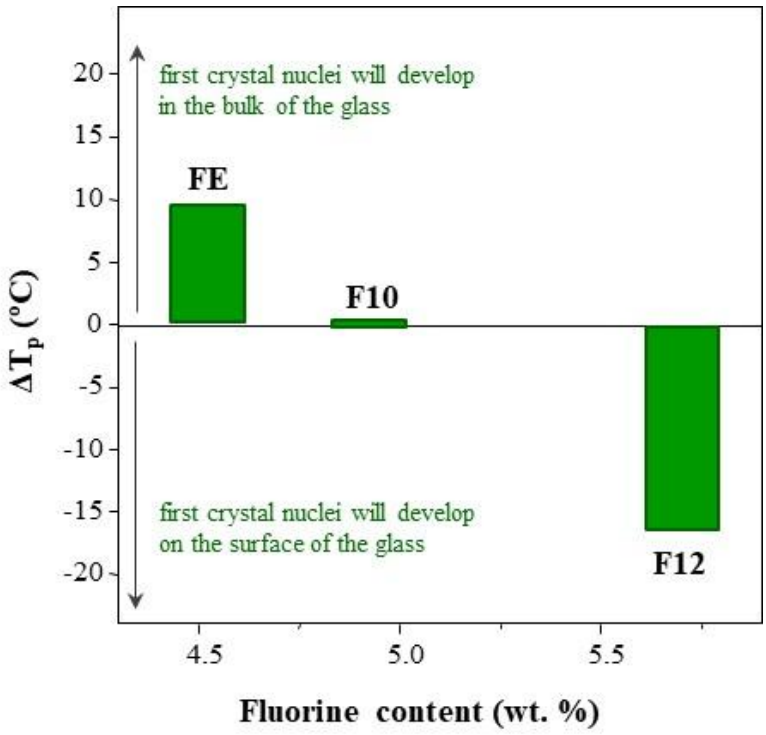

Figure 2. Evolution of ΔT_p with the fluorine content for each glass composition.

ΔT_p clearly decreases when the fluorine content increases, which indicates a variation in spatial location where the crystal nuclei are developed in the early stages of the crystallization process. Thus, the devitrification of the FE glass with $\Delta T_p > 0$ begins with the growth of crystals in the body of the glass particles, whereas in the F12 glass with $\Delta T_p < 0$, the first crystal nuclei develop on the surface of the glass grains. From a theoretical point of view, surface crystallization is always present in glass devitrification because of close to or on the surface of glass particles, both thermodynamic and kinetic barriers for nucleation are typically lower than bulk values, causing a predominance of surface nucleation; *ca.* 90% of silicate glasses display only surface crystallization[36].

The preferred nucleation mechanism (volume or surface) by which the glass crystallizes can be evaluated from the reduced glass transition temperature T_{gr}, which is the ratio between the glass transition temperature and the melting temperature ($T_{gr} = T_g / T_m$)[36]. Therefore, $T_{gr} < 0.58$ indicates the primacy of volume crystallization (homogeneous or heterogeneous nucleation), whereas $T_{gr} > 0.60$ indicates that the devitrification process occurs through a surface (mostly heterogeneous) crystallization mechanism[37-39]. Figure 3 shows the values of T_{gr} with fluorine content for the different glass compositions in both coarse and fine (<63 µm) samples.

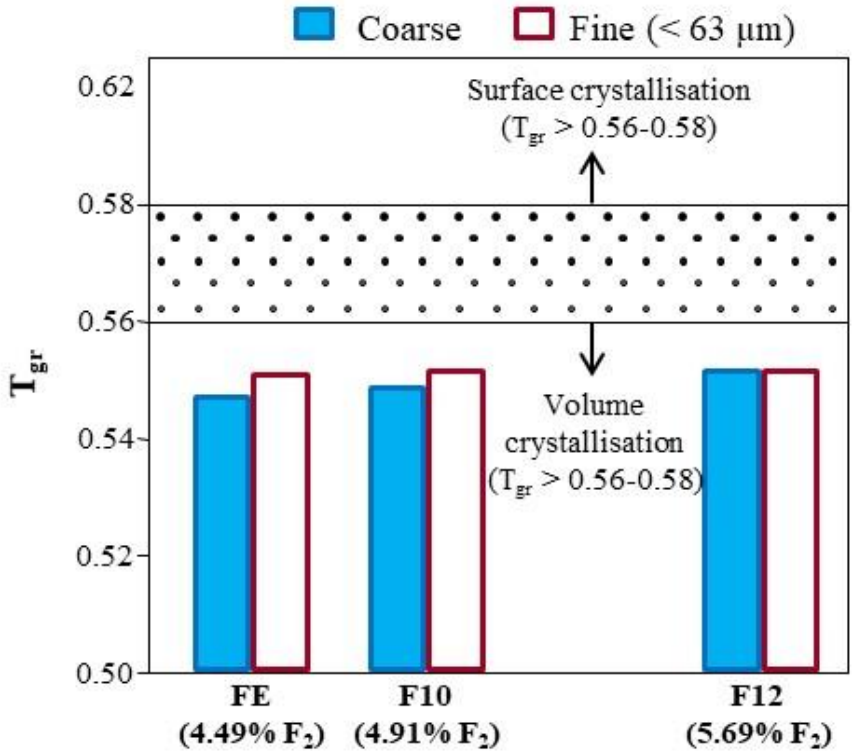

Figure 3. Values of T_{gr} for FE, F10 and F12 glasses from both coarse and fine (<63 µm) glass particles.

All glass compositions are in the graph section that corresponds to a prevalent volume crystallization mechanism. Moreover, fine and coarse glass samples depicts similar T_{gr} values, which is indicating that, contrary to what happens in other glass systems[40], surface crystallization contribution in F-phlogopite glasses does not became more significant when glass particle size decreases and the surface to volume ratio increases. Therefore, the evaluation of ΔT_p and T_{gr} suggests that the devitrification of these F-phlogopite-based glasses mainly proceeds through a volume crystallization mechanism. Nevertheless, the increase in fluorine content in the glass composition changes the location of the first developed crystals in the early stages: from the internal volume of the glass particle to surface sites.

To verify these results, samples of glass frit of the different compositions were subjected to a heat treatment at 850°C for 10 minutes to promote the beginning of crystal growth. Figure 4 presents the X-ray spectra of the heat treated glass samples. According to the patterns, the crystallization process of the studied frits proceeds through the precipitation of F-phlogopite (JCPDS file No. 16-352).

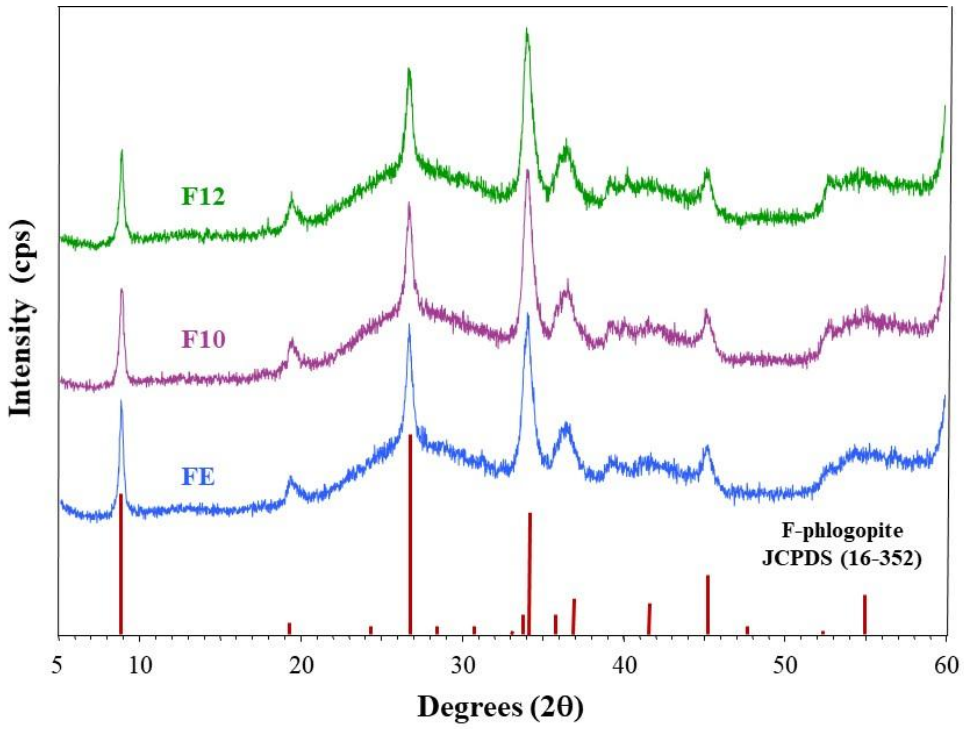

Figure 4. XRD patterns for FE, F10 and F12 glass samples heat treated at 850°C for 10 minutes.

Figure 5 shows the microstructure observed with FESEM on the cross section of the heat-treated FE glass. Fig. 5(a) clearly confirms that the FE glass devitrifies through a preferential volume crystallization mechanism, which develops a glass-ceramic material composed of tiny crystals that are uniformly distributed throughout the entire volume of the material (Fig. 5(b)). Although a crystalline shell on the surface of the glass particles is not observed, there is evidence of heterogeneous surface crystallization to a lesser extent in Fig. 5(c,d), which shows the formation of crystals over existing internal cracks in the original glass frit particle. The EDS analyses that were performed on such crystals (Fig. 5(e)) illustrate the development of F-phlogopite; crystals (C) show higher F, Mg and K ion contents than the glass-ceramic body (B), which is enriched in Si and Al. Schmelzer et al.[41] suggested that the degree of catalytic activity of the glass surface in stimulating crystallization highly depended on its roughness, so that the energy required to form a crystal on the smooth surface of a glass particle is greater than that for its progress on a fracture surface with multiple corners and edges.

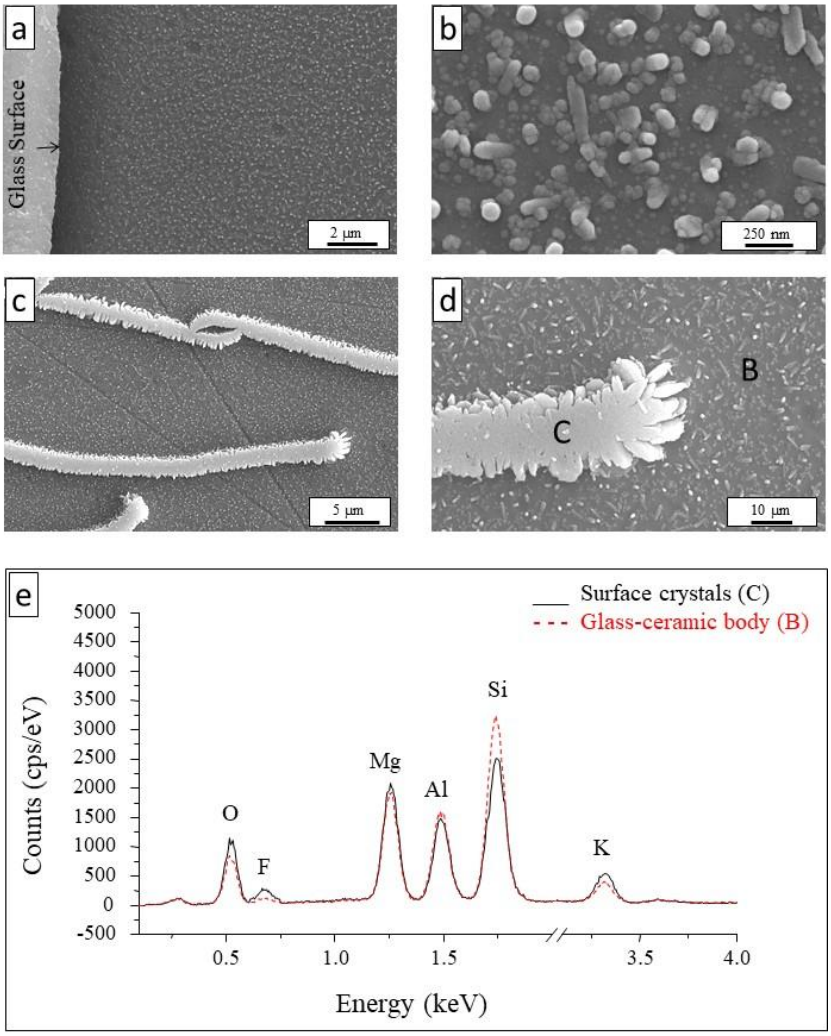

Figure 5. Secondary electron images on cross section of etched FE glass heat-treated at 850°C for 10 minutes. a) General SEM image showing the absence of a crystalline shell on the surface of the glass particle; b) High-magnification image on an inner region showing volume crystallization mechanism; c) and d) Surface crystallization over existing cracks and e) Energy dispersive X-ray spectra of F-phlogopite crystals (C) and glass-ceramic body (B).

This hypothesis has been confirmed in cordierite and diopside glasses[36,42], and it is also verified when the FE glass is subjected to a supplementary heat treatment at 850°C for 10 min (Figure 6). It is expected that under isothermal conditions, the surface crystalline layer tends to shift to the interior of the glass particle as the time of heat treatment increases. In fact, the additional treatment promotes the development of crystals at the surface of frit particles (Fig. 6(a)), and small flakes or pseudo-hexagonal crystals with an average size of 2.5 x 0.8 µm are detected using FESEM (Fig. 6(b)). Fig. 6(c) shows a FESEM image with the elemental mapping of F, Mg, K, Si and Al. F-phlogopite crystals are clearly identified based on the color dissimilarities caused by different concentrations of these ions among the surface crystals and glass-ceramic

body. Table II shows the EDS analyses collected from crystals developed over internal cracks (Fig. 5(c,d)) and at the surface of frit particles (Fig. 6). Regardless of the position at which they are located, the crystals developed at the beginning of FE glass crystallization have chemical composition close to stoichiometric F-phlogopite.

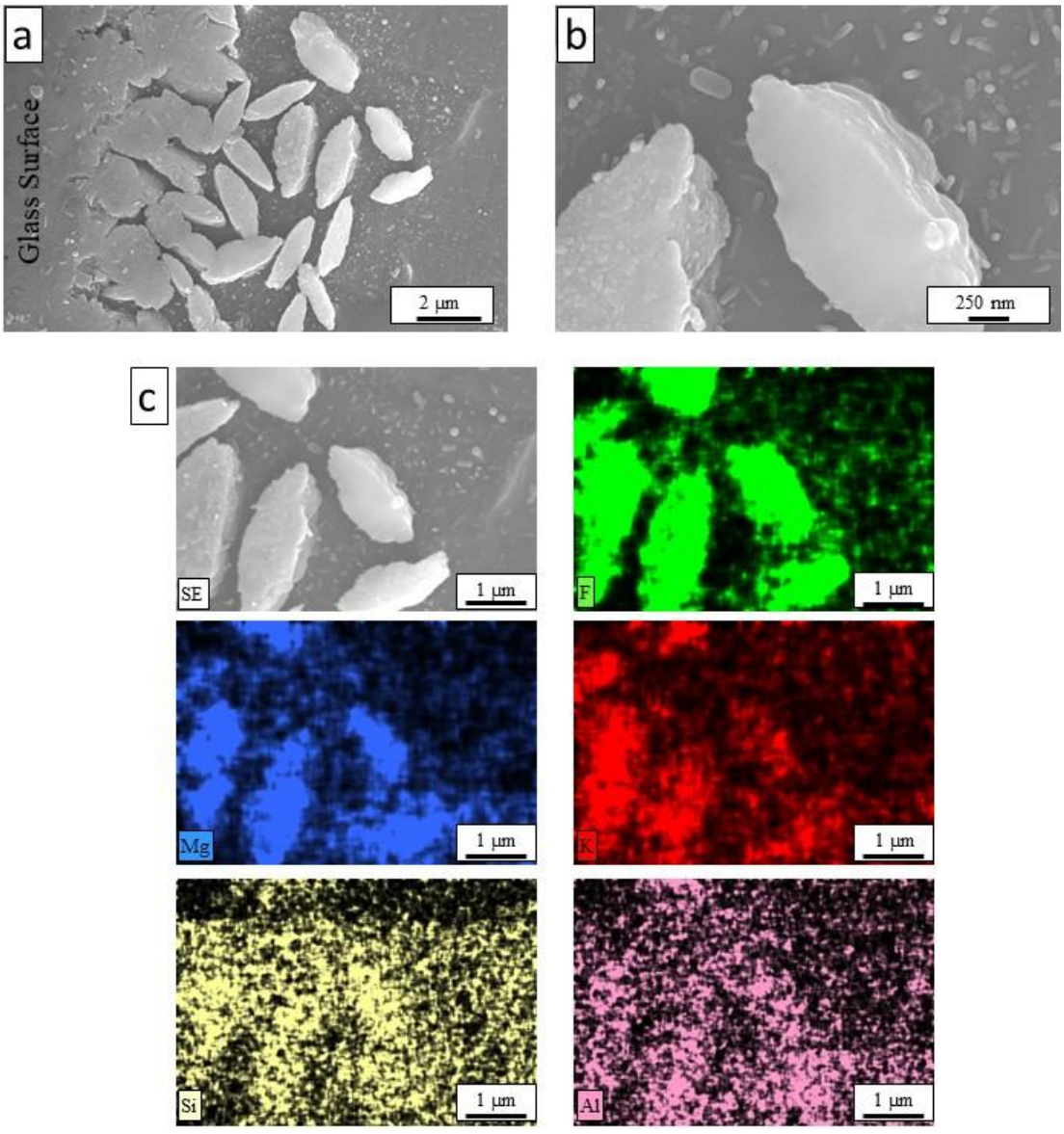

Figure 6. Secondary electron images (a and b) and elemental mapping (c) on cross section of etched FE glass heat-treated at 850°C for 10+10 minutes. a) General SEM image showing the occurrence of a crystalline shell on the surface of the glass particle; b); Detail of flakes-like F-phlogopite crystals c) F (green color), Mg (blue color), K (red color), Si (yellow color) and Al (pink color).

Table 2. EDS analyses (wt. %) collected from crystals developed over internal cracks and at the surface of frit particles.

		SiO_2	Al_2O_3	MgO	K_2O	F_2
Internal cracks	1	41.31	18.11	24.81	9.32	6.46
	2	43.80	18.10	23.70	8.56	5.84
	3	42.45	18.57	24.20	8.96	5.82
	4	41.33	18.23	24.62	9.44	6.38
	5	43.65	18.15	23.82	8.36	6.02
	Average	42.51	18.23	24.23	8.93	6.11
	SD*	1.20	0.20	0.48	0.47	0.30
Surface	1	42.85	19.01	25.10	6.48	6.56
	2	43.00	19.09	25.06	5.83	7.02
	3	43.71	18.33	24.32	7.48	6.16
	4	45.42	18.93	23.79	6.22	5.63
	5	45.30	18.80	23.87	6.22	5.80
	Average	44.06	18.83	24.43	6.45	6.23
	SD*	1.23	0.30	0.63	0.62	0.57
Stoichiometric F-phlogopite		41.24	11.63	27.66	10.77	8.69

* SD = standard deviation

Figures 7 and 8 reveal that the volume crystallization (homogeneous nucleation) is also the preferred devitrification mechanism in the F10 and F12 glasses; however, in this case, a thermal treatment at 850°C for 10 minutes is sufficient to promote crystal growth on the surface of the glass particle (heterogeneous nucleation). A crystallization shell is developed, whose depth significantly increases with increasing fluoride content in the glass composition: from 1-3 µm thick in the F10 glass (Fig. 7(a,b)) to 20-30 µm thick in the F12 glass (Fig. 8(a)). Therefore, increasing the fluoride content in the glass composition enhances the extent of heterogeneous surface crystallization. This effect is also evident in the crystallization front, where crystals arose along the traces of former internal cracks, and the average crystal thickness increases from ≈1.6 µm in FE glass (Fig. 5(c)) to ≈8.2 µm in the F10 glass (Fig. 7(c)).

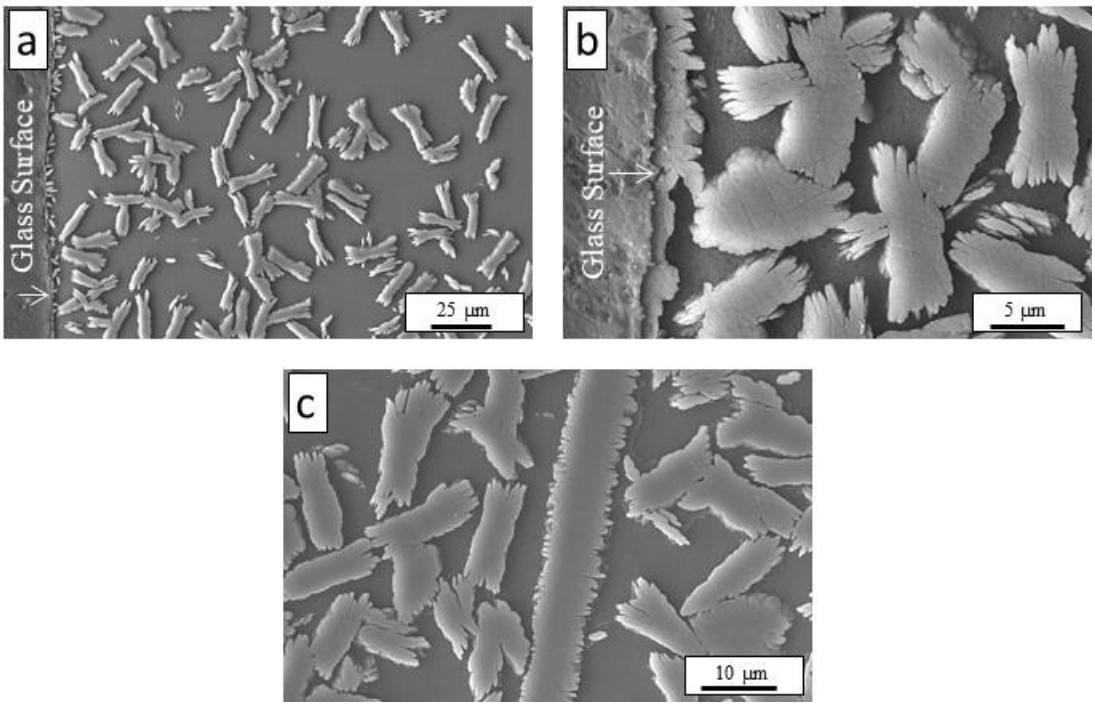

Figure 7. Secondary electron images on cross section of etched F10 glass heat-treated at 850°C for 10 minutes. a) and b) General SEM image showing the presence of a crystalline shell on the surface of the glass particle; c) High-magnification image on an inner region showing volume crystallization mechanism and surface crystallization over existing cracks.

The morphology of F-phlogopite crystals, which developed in the entire volume of the F12 glass after the thermal treatment at 850°C for 10 min, is shown in Fig. 8(a) and observed in details in Fig. 8(b). The micrograph shows that these crystals are actually clusters of small flakes or sheets of F-phlogopite with similar dimensions to those developed on the surface of the frit particles. These crystals agglomerate in crystalline sheaf-like formations. A comparison of Figs. 7(a) and 8(a) shows that the number of crystals by unit volume decreases by increasing the fluorine content in the glass composition, which results in fewer but larger crystalline clusters. Thus, the density of the crystalline clusters in the thermal-treated F10 is $13.6x10^3$ crystals/mm^2, with an average size of ≈12 µm long and ≈5 µm wide at the central of the cluster, whereas in the F12 glass, the density of crystalline clusters is ≈$1.5x10^3$ crystals/mm^2, with an average size of ≈35-50 µm long and 8 µm wide.

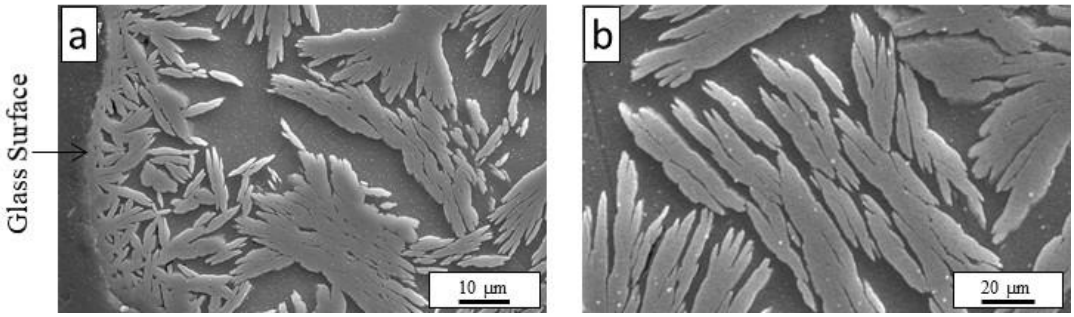

Figure 8. Secondary electron images on cross section of etched F12 glass heat-treated at 850°C for 10 minutes.

FESEM observations have shown that F-phlogopite crystals are immersed in a glass-ceramic matrix comprised by tiny granular crystals. Figure 9 shows the microstructure of the glass-ceramic matrix in heat-treated FE, F10 and F12 glasses. It is observed the occurrence of small granules showing an average diameter of ≈30-45 nm, which are grouped with each other, forming clusters whose dimensions vary with the fluorine content in the parent glass composition. Thus, these clusters increase from an average size of ≈70 nm in FE to ≈150-180 nm in F12 glass-ceramic.

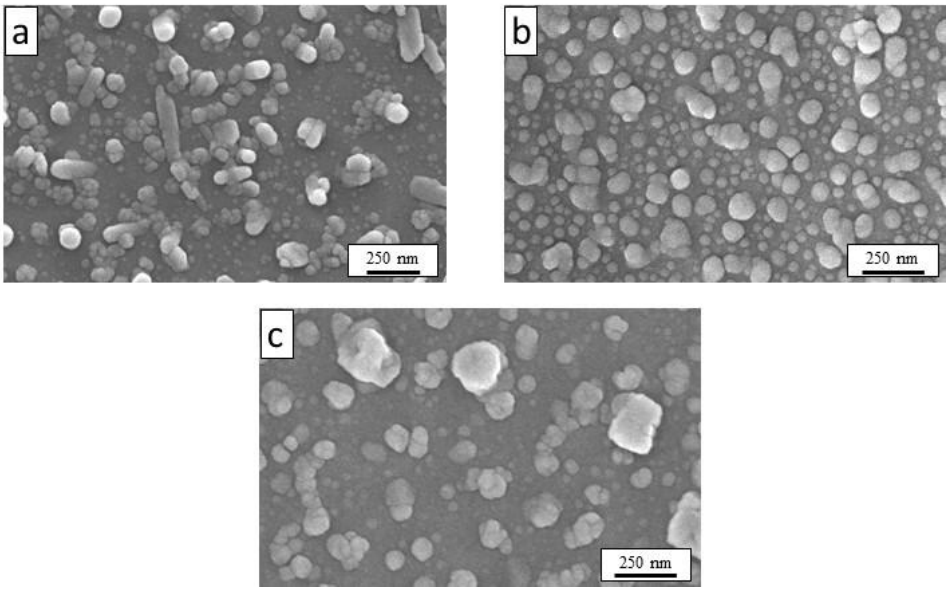

Figure 9. Secondary electron images of the glass-ceramic matrix in the glass samples heat-treated at 850°C for 10 minutes: a) FE, b) F10 and c) F12 glass.

The occurrence of two different crystal shapes, namely spheres and flakes, has been previously reported in mica glass ceramics[43]. According to Grossman[44], the dissimilar morphologies indicate that the crystals are in a different stage of crystallization. He stated that in an early stage of growth, phase separation leads to the crystallization of quasi-spherical mica grains (≈40 nm in diameter). Afterwards, at higher temperature the mica grains recrystallize by grouping into larger booklets with blocky appearance. To verify the occurrence of phase separation, the microstructure of the original glasses were observed by FESEM on fresh fractured surfaces subjected to chemical etching. The study revealed the existence of a texture indicative of liquid-liquid immiscibility in all glasses[41]. Silicate melts with alkaline earth elements show a high tendency to undergo phase separation during cooling. In the development of phase separation, the occurrence of elements in small amounts in the glass composition plays an important role. The effect of these additives is mainly attributed to the fact that they can cause either substantial variation in the interfacial tension of the phase where they are concentrated or a modification in the glass structure. These changes may give rise to phases at lower viscosities and high rates of ionic diffusion, so that phase separation can be further developed. Consequently, the tendency of phase separation in glasses in which part of the oxygen ions are substituted by fluorine[45] is increased.

Figure 10 shows the microstructure of the fracture surface of F-phlogopite glasses. It is evident the occurrence of spherical droplets with poor connectivity, which are embedded in a continuous matrix of a second phase. This morphology is characteristic of a phase separation process by a mechanism of nucleation and growth, also known as "binodal decomposition"[46]. Although droplet density is high in all glasses, its size varies with the fluorine content in the glass composition. Thus, FE glass (Fig. 10(a)) shows a phase separation finer, with more uniform size droplets and average diameter of 50 nm, whereas in F12 (Fig. 10(b)) the drop size increases and varies in the range ≈80-130 nm. Elements of the 7th group of the periodic table (especially F, Cl and Br) when introduced into silicate or borate glasses, as a rule strongly increase the phase separation tendency existing in the respective plain basic glasses[45]. In mica glasses, droplets enriched in Mg, K and F precipitate in a silicate matrix phase[47]. Therefore, in the studied glasses fluorine ions lead to volume crystallization through homogeneous nucleation from liquid-liquid immiscibility.

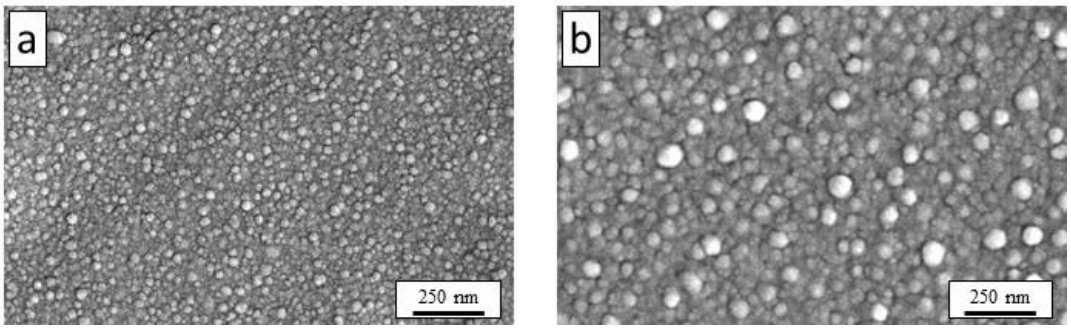

Figure 10. Secondary electron images on the fresh fracture surface of a) FE glass and b) F12 glass.

5. Conclusions

F-phlogopite-based glasses in the SiO_2-MgO-K_2O-F system were evaluated using DSC and FESEM to establish the effect of the fluorine content on the preferential crystallization mechanism and crystal growth in the early stages of devitrification. The results show that both surface and volume mechanisms contribute to the crystallization of F-phlogopite glasses. Nevertheless, these glasses preferentially devitrify by a volume crystallization mechanism (internal homogeneous nucleation), although an increase in fluorine content leads to a modification in the location of the first developed crystals from the internal volume of the glass particle to the surface sites.

The evaluation of the microstructure of parent glasses and glass-ceramics suggest that the bulk crystallization of F-phlogopite proceeds through a phase separation process in the base glass through a mechanism of nucleation and growth.

Acknowledgements

The authors would like to acknowledge Mrs. P. Díaz for her technical support in the experimental study. R. Casasola and J.M. Pérez express their gratitude to the Spanish National Research Council (CSIC) for their contract through the JAE Program (JAEPre-08-00456 and JAEDoc-08-00362, respectively), which is co-financed by the European Social Fund. The financial support through the projects MAT 2006-05977 and MAT2013-40477-P is also recognized.

References

1. P. W. McMillan, *Glass-Ceramics*, 2nd ed. Academic Press Inc, London, 1979.

2. Z. Strnad, *Glass-Ceramic Materials*, Elsevier, Amsterdam, 1986.
3. W. Höland and G. Beall, *Glass-Ceramic Technology*, The American Ceramic Society, Westerville, Ohio, 2002.
4. G. Partridge, "An overview of glass ceramics. II: Joining, minor applications and the future," *Glass Technol*., **35** [4] 116-127 (1994).
5. P. F. James, "Glass ceramics: new compositions and uses," *J Non-Cryst. Solids*, **181** [1-2] 1-15 (1995).
6. W. Pannhorst, "Glass ceramics: state-of-the-art," *J Non-Cryst. Solids*, **219** [1] 198-204 (1997).
7. W. A. Deer, R. A. Howie and J. Zussman, *An Introduction to Rock-Forming Minerals*, 2nd ed. Pearson Education Ltd, London, 1996.
8. A. Faeghi-Nia and T. Ebadzadeh, "Fabrication of machinable phlogopite-glass composite using microwave processing," *Ceram. Int*., **38** [4] 2653-2658 (2012).
9. M. Ghasemzadeh and A. Nemati, "Role of MgF_2 on properties of glass-ceramics," *Bull. Mater. Sci*., **35** [5] 853-858 (2012).
10. Z. Khalkhali, Z. Hamnabard, B. Eftekhari Yekta, M. Nasiri, E. Khatibi, "Sintering Behavior and Machinability of Phlogopite Glass Ceramics Containing Fe_2O_3," *J. Mater. Eng. Perform.*, **22** [2] 528-535 (2013).
11. A. Faeghi-Nia, V. K. Marghussian, E. Taheri-Nassaj, M. J. Pascual and A. Durán, "Pressureless Sintering of Apatite/Wollastonite-Phlogopite Glass-Ceramics," *J. Amer. Ceram. Soc*., **92** [9] 1514-1518 (2009).
12. P. Alizadeh, B. EftekhariYekta and T. Javadi, "Preparation of machinable bioactive mica diopside-fluoroapatite glass-ceramics," *Ad.v Appl. Ceram.*, **109** [1] 56-61 (2010).
13. K. Chyung, and S.B. Dawes, "Fluoromica coated nicalon fiber-reinforced glass-ceramic composites," *Mater. Sci. Eng. A.*, **162** [1-2] 27-33 (1993).
14. M. Romero, J. Ma. Rincón and A. Acosta, "Development of mica glass-ceramic glazes," *J. Amer. Ceram. Soc*., **87** [5] 819-823 (2004).
15. A. Mallik, A. Basumajumdar, P. Kundu and P. K. Maiti, "Some studies on nucleation, crystallization, microstructure and mechanical properties of mica glass-ceramics in the system $0.2BaO{\cdot}0.8K_2O{\cdot}4MgO{\cdot}Al_2O_3{\cdot}6SiO_2{\cdot}2MgF_2$," *Ceram. Int.*, **39** [3] 2551-2559 (2013).
16. A. Mallik, P. K. Maiti, P. Kundu, and A. Basumajumdar, "Influence of B_2O_3 on Crystallization Behavior and Microstructure of Mica Glass-Ceramics in the System $BaO{\cdot}4MgO{\cdot}Al_2O_3{\cdot}6SiO_2{\cdot}2MgF_2$," *J. Amer. Ceram. Soc.*, **95** [11] 3505-3508 (2012).
17. P. K. Maiti, A. Mallik, A. Basumajumdar and P. Guha, "Influence of barium oxide on the crystallization, microstructure and mechanical properties of potassium fluorophlogopite glass-ceramics," *Ceram. Int.*, **38** [1] 251-258 (2012).

18. P. K. Maiti, A. Mallik, A. Basumajumdar and K. *J.* Das,"Some studies on nucleation, crystallization and microstructural behaviour of mica glass-ceramics in the system $0.8BaO{\cdot}0.2K_2O{\cdot}4MgO{\cdot}Al_2O_3{\cdot}6SiO_2$·," *Ind. Chem. Soc*., **88** [10] 1509-1515 (2011).
19. P. Naresh, G. N. Raju, Y. Gandhi, M. Piasecki and N.Veeraiah, "Insulating and Other Physical Properties of CoO-Doped Zinc Oxyfluoride-Borate Glass-Ceramics," *J. Amer. Ceram. Soc*., **98** [2] 413-422 (2015).
20. C. J. Alvarez, R. L. Leonard, S. K. Gray, J. A. Johnson and A. K. Petford-Long, "Structural and Kinetic Analysis of $BaCl_2$ Nanocrystals in Fluorochlorozirconate Glass-Ceramics," *J. Amer. Ceram. Soc*., **98** [4] 1099-1104 (2015).
21. J. H. Lopes, A. Magalhaes, I. O. Mazali and C. A. Bertran, "Effect of Niobium Oxide on the Structure and Properties of Melt-Derived Bioactive Glasses," *J. Amer. Ceram. Soc*., **97** [12] 3843-3852 (2014).
22. L. B. de Mello, F. A. Sigoli and I. O. Mazali, "Structural and Optical Properties of Erbium and Ytterbium Codoped Germanoniobophosphate Glasses," *J. Amer. Ceram. Soc*., **97** [8] 2462-2470 (2014).
23. M. H. Imanieh, I. R. Martin, B. E. Yekta, J. Gonzalez-Platas and A. H. Creus," Investigation on Crystallization and Optical Properties of $Ca_{1-x}La_xF_{2+x}$ Glass- Ceramics," *J. Amer. Ceram. Soc*., **97** [3] 782-788 (2014).
24. C. J. Alvarez, Y. Z. Liu, R. L. Leonard, J. A. Johnson and A. K. Petford-Long, "Nanocrystallization in Fluorochlorozirconate Glass-Ceramics," *J. Amer. Ceram. Soc*., **96** [11] 3617-3621 (2013).
25. Lj. Radonjić and Lj. Nikolić, "The effect of fluorine and concentration on the crystallization of machinable glass-ceramics," *J. Eur. Ceram. Soc*., **7** [1] 11-16 (1991).
26. M. Ghasemzadeh and A. Nemati, "Role of MgF_2 on properties of glass-ceramics," *Bull. Mater. Sci.*, **35** [5] 853–858 (2012).
27. P. K. Maiti, A. Mallik, A. Basumajumdar and P.Kundu,"Influence of fluorine content on the crystallization and microstructure of barium fluorphlogopite glass-ceramics," *Ceram. Int.*, **36** [1] 115–120 (2010).
28. R. Casasola, J. M. Pérez and M. Romero, *J. Therm. Anal. Calorim.*, in press (available at http://link.springer.com/article/10.1007/s10973-015-4524-1).
29. M. Velez, J. Smith and R. E. Moore, "Refractory Degradation in Glass Tank Melters. A Survey of Testing methods," *Cerâmica*, **43** [283-284] 180-184 (1997).
30. A. A. Kiprianov and N.M. Pankratova, "Investigation of fluorine binding by lithium barium alkali silicate glass," *Glass Phys. Chem*., **40** [2] 133–137 (2014).
31. A. A. Kiprianov and N. G. Karpukhina, "Oxyhalide silicate glasses," *Glass Phys. Chem*., **32**[1] 1–27 (2006).

32. N. G. Karpukhina, U. Werner-Zwanziger, J. W. Zwanziger and A. A. Kiprianov, "Preferential binding of fluorine to aluminum in high peralkaline aluminosilicate glasses," *J. Phys. Chem. B.*, **111**[35] 10413-10420 (2007).
33. A. A. Kiprianov, E. A. Pyatina and I. S. Ivanovskaya, "Specific Features of Halogen Binding in Binary Alkali Silicate Glasses," *Glass. Phys. Chem.*, **34** [5] 519–526 (2008).
34. A. A. Kiprianov and I. A. Ponomarev, "Study of the principles of fluorine fixation in melts and glass with polar groups," *Glass. Phys. Chem.*, **41**[2] 145–150 (2015).
35. R. L. Thakur and S. Thiagarajan, "Studies in catalyzed crystallization of glasses: A DTA method," *Cent. Glass Ceram. Res. Inst. Bull.*, **13** [2] 33-45 (1966).
36. E. D. Zanotto and V. M. Fokin, "Recent studies of internal and surface nucleation in silicate glasses," *Philos. Trans. R. Soc. A-Math. Phys. Eng. Sci.*, **361** [1804] 591-613 (2003).
37. P. F. James, in *Glasses and Glass- Ceramics*, Chapman and Hall, London, 1989.
38. E. D. Zanotto,"Isothermal and adiabatic nucleation in glass," *J. Non-Cryst. Solids*, **89** [3] 361-370 (1987).
39. E. D. Zanotto and M. C. Weinberg,"Trends in homogeneous crystal nucleation in oxide glasses," *Phys. Chem. Glasses*, **30** [5] 186-192 (1989).
40. L. E. Marques, A. M. C. Costa, M. C. Crovace, A. C. M. Rodrigues and A. A. Cabral, "Influence of particle size on nonisothermal crystallization in a lithium disilicate glass," J. *Am. Ceram. Soc.*, **98** [3] 774–780 (2015).
41. J. Schmelzer, J. Möller, I. Gutzow, R. Pascova, R. Müller and W. Pannhorst, "Surface-energy and structure effects on surface crystallization," *J. Non-Cryst. Solid*s, **183** [3] 215-233 (1995).
42. R. Müller, "Surface nucleation in cordierite glass," *J. Non-Cryst. Solid*s, **219** 110-118 (1997).
43. P. Alizadeh, B. E. Yekta and J.Tannaz, "Sintering behavior and mechanical properties of the mica-diopside machinable glass-ceramics," *J. Eur. Ceram. Soc.*, **28** [8] 1569–1574 (2008).
44. D. G. Grossman, "Machinable glass-ceramics based on tetrasilicic mica," *J. Amer. Ceram. Soc.*, **55** [9] 446-449 (1972).
45. W. Vogel, "Phase separation in glass," *J. Non-Cryst. Solids*, **25** [1] 170-214 (1977).
46. B. R. Wheaton and A. G. Clare, "Evaluation of phase separation in glasses with the use of atomic force microscopy," *J. Non-Cryst. Solids*, **353**, 4767-4778 (2007).
47. S. A. M. Abdel-Hameed, N. A. Ghoniem, E. A. Saad and F. H. Margha, "Effect of fluoride ions on the preparation of transparent glass ceramics based on crystallization of barium borates," *Ceram. Int.*, **31** [4] 499-505 (2005)